Contents lists available at ScienceDirect

Current Research in Pharmacology and Drug Discovery

Hypoxia represses early responses of prostate and renal cancer cells to YM155 independent of HIF-1α and HIF-2α

David Danielpour [a,b,c,*], Sarah Corum [a], Scott M. Welford [d,e], Eswar Shankar [a,1]

[a] Case Comprehensive Cancer Center Research Laboratories, The Division of General Medical Sciences-Oncology, Case Western Reserve University, Cleveland, OH, 44106, USA
[b] Department of Pharmacology, Case Western Reserve University, Cleveland, OH, 44106, USA
[c] Department of Urology, University Hospitals of Cleveland, Cleveland, OH, 44106, USA
[d] Department of Radiation Oncology, Case Western Reserve University, Cleveland, OH, 44106, USA
[e] Department of Radiation Oncology, University of Miami, FL, 33136, USA

ARTICLE INFO

ABSTRACT

The imidazolium compound Sepantronium Bromide (YM155) successfully promotes tumor regression in various pre-clinical models but has shown modest responses in human clinical trials. We provide evidence to support that the hypoxic milieu of tumors may limit the clinical usefulness of YM155. Hypoxia (1% O_2) strongly (>16-fold) represses the cytotoxic activity of YM155 on prostate and renal cancer cells in vitro. Hypoxia also represses all early signaling responses associated with YM155, including activation of AMPK and retinoblastoma protein (Rb), inactivation of the mechanistic target of rapamycin complex 1 (mTORC1), inhibition of phospho-ribosomal protein S6 (rS6), and suppression of the expression of Cyclin Ds, Mcl-1 and Survivin. Cells pre-incubated with hypoxia for 24 h are desensitized to YM155 even when they are treated with YM155 under atmospheric oxygen conditions, supporting that cells at least temporarily retain hypoxia-induced resistance to YM155. We tested the role of hypoxia-inducible factor (HIF)-1α and HIF-2α in the hypoxia-induced resistance to YM155 by comparing responses of YM155 in VHL-proficient versus VHL-deficient RCC4 and 786-O renal cancer cells and silencing HIF expression in PC-3 prostate cancer cells. Those studies suggested that hypoxia-induced resistance to YM155 occurs independent of HIF-1α and HIF-2α. Moreover, the hypoxia mimetics deferoxamine and dimethyloxalylglycine, which robustly induce HIF-1α levels in PC-3 cells under atmospheric oxygen, did not diminish their early cellular responses to YM155. Collectively, our data support that hypoxia induces resistance of cells to YM155 through a HIF-1α and HIF-2α-independent mechanism. We hypothesize that a hypothetical hypoxia-inducer factor (HIF-X) represses early signaling responses to YM155.

1. Introduction

A hallmark of tumors is their hypoxic niche, developed as their oxygen consumption exceeds vascular supply (Brown, 1990; Sorensen and Horsman, 2020). Tumors survive under such low oxygen levels by at least three mechanisms: 1) Tumors "re-wire" their metabolism to reduce their consumption of oxygen by inhibiting oxidative phosphorylation, accompanied by compensatory increased glucose uptake and glycolysis (Shukla et al., 2018). 2) Tumor cells and their associated stroma are encouraged to produce and secrete vascular endothelial growth factor (VEGF), which promotes the growth of new blood vessels (angiogenesis) (Detmar et al., 1997; Baek et al., 2000). 3) Tumor cells are

re-programmed to become more migratory and invasive, enabling their entry into a less hostile environment (Osinsky et al., 2009; Jiang et al., 2011). These and other mechanisms empower tumors to progress to a state of increased aggressiveness accompanied by the acquisition of resistance to various therapies, including radiation therapy (Sorensen and Horsman, 2020) and chemotherapy (Jiang et al., 2011, 2019).

Despite the significant impact of hypoxia on tumor cell responses, most initial in vitro drug screening and testing strategies rely on conditions that expose cells to near atmospheric levels of O_2 and are thereby hyperoxic with respect to the in vivo environment of tumors (Griner et al., 2018; Das et al., 2015). Technological and conceptual advances within the past decade have enabled a better understanding of the role of the

* Corresponding author. Wolstein Research Building, Room 3-532, 2103 Cornell Avenue, Cleveland, OH, 44106, USA.
E-mail address: dxd49@case.edu (D. Danielpour).
[1] Current affiliation: Medical Oncology Division, Wexner Medical Center, Ohio State University, Columbus, OH 43210.
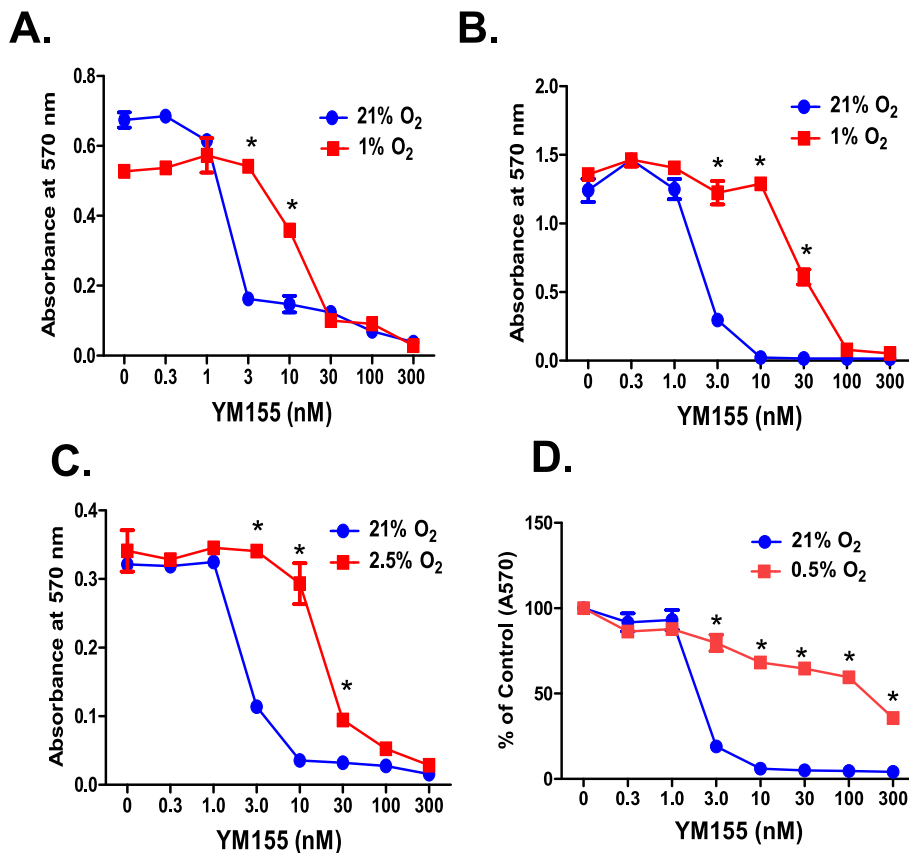
Fig. 1. Effect of hypoxia on the suppression of PC-3 cell growth. PC-3 cells were allowed to attach to 12-well dishes for 24 h under normal atmospheric oxygen (21% O_2) and then treated with various doses of YM155 or vehicle for 72 h in 1% or 21% O_2 **(A)**, pre-incubated for 24 h in 1% or 21% O_2 before treatment with various doses of YM155 or vehicle for 72 h in 1% or 21% O_2 **(B)**, pre-incubated for 24 h in 2.5% or 21% O_2 before treatment with various doses of YM155 or vehicle for 72 h in 2.5% or 21% O_2 **(C)**, and pre-incubated for 24 h in 5% or 21% O_2 before treatment with various doses of YM155 or vehicle for 72 h in 5% or 21% O_2 **(D)**. Cell growth was assessed by crystal violet staining (A570 nm) as described in Materials and Methods. Data points represent the average of triplicate determinations (biological replicates) ± SE. Statistical significance (p-values) was determined by Student's t-test (two-tailed). *$p < 0.01$.

Table 1

The effect of hypoxia on growth suppression of PC-3 cells by YM155 was assessed by crystal violet growth assay as in Fig. 1 and described in the Material and Methods. The IC$_{50}$ values were assessed by dose-response curves using GraphPad Prism software and represent the average of triplicate biological determinations ± SE.

Hypoxia Incubation conditions	IC50 (nM)Normoxic (21% O2)	IC50 (nM) Hypoxic	% O2
Co-treatment incubation	1.7 ± 0.1	11.86 ± 0.52	1%
Pre-treatment incubation	1.82 ± 0.14	26.8 ± 2.7	1%
Pre-treatment incubation	2.0 ± 0.08	125 ± 3.9	0.5%
Pre-treatment incubation	1.7 ± 0.05	22.14 ± 1.7	2.5%
Pre-treatment incubation	2.2 ± 0.12	2.4 ± 0.1	5%

Table 2

The impact of hypoxia on the cytostatic effect of various prostate cancer cell lines was assessed by crystal violet growth assay as in Fig. 1 and described in Materials and Methods. All cell lines were pre-treated for 24 h with 1% O2 or 21% O2 before the addition of various doses of YM155 or vehicle control and cells were cultured in their respective growth conditions for an additional 72 h before crystal violet staining. The IC$_{50}$ values were assessed by dose-response curves using GraphPad Prism software and represent the average of triplicate biological determinations ± SE.

Cell Line	IC50 (nM)Normoxic	IC50 (nM)Hypoxic	Fold Change
PC-3	1.82 ± 0.14	26.8 ± 2.6	14.9
DU-145	3.95 ± 0.11	58.9 ± 2.0	15
C4-2	8.7 ± 0.6	163.9 ± 18.7	19.4
LNCaP	44 ± 5.4	>300	>6.8
22RV1	8.15 ± 0.43	202.5 ± 14.8	24.8

hypoxic milieu as a predictor of tumor aggressiveness and their accompanying responses to therapies. Along these lines, in the current study,

we explored the effect of hypoxia on the activity of Sepantronium Bromide (YM155), a potent anti-cancer cationic imidazolium compound. Our findings support that levels of hypoxia encountered in tumors robustly impact the therapeutic effectiveness of YM155.

YM155 is a potent inducer of cell death as assayed on a broad spectrum of human cancer cell lines *in vitro* (Nakahara et al., 2007, 2011). Remarkably, this drug also robustly promotes the regression of a variety of human tumor xenografts in immunocompromised mice without causing overt host systemic toxicity or weight loss (Nakahara et al., 2007, 2011). YM155 was discovered and first reported as an inhibitor of the survivin gene promoter in prostate cancer cells (Nakahara et al., 2007). Subsequent studies found this drug to target cancer cells through other mechanisms including, loss of Mcl-1 (Wagner et al., 2014; Feng and Ueda, 2013; Tang et al., 2011), targeting Akt, ERK, PI3K and STAT3 (Zhang et al., 2018; Na et al., 2012), degradation of EGFR (Na et al., 2012), DNA damage response (Chang et al., 2015; Glaros TG et al., 2012; Wani et al., 2018; Xu et al., 2021; Wani et al., 2021), and unfolded protein response (Wagner et al., 2014). YM155 reportedly induces apoptosis (Iwasa T et al., 2008; Iwasa et al., 2010; Tao et al., 2012; Feng et al., 2013) and autophagy (Wang et al., 2011, 2014). Recent work from our group focusing on understanding the early signaling responses driven by YM155 revealed that YM155 rapidly (within 30 min) activates AMPK signaling, leading to activation of ULK1, suppression of mTORC1, and corresponding inhibition of global protein synthesis (Danielpour et al., 2019). Given that cellular uptake of YM155 occurs by cationic transporters, a process that delays its availability to intracellular targets compared to cell-permeable compounds (Minematsu et al., 2009), we postulated that the impact of YM155 on AMPK/mTORC1/ULK1 represented early signaling responses compared to downstream responses such as loss of Survivin and Mcl-1 expression (Danielpour et al., 2019).

YM155 was tested in phase I and II clinical trials of castrate-resistant prostate cancer (Tolcher et al., 2011; Aoyama et al., 2013), non-small-cell lung cancer (Giaccone et al., 2009), unresectable stage III or IV
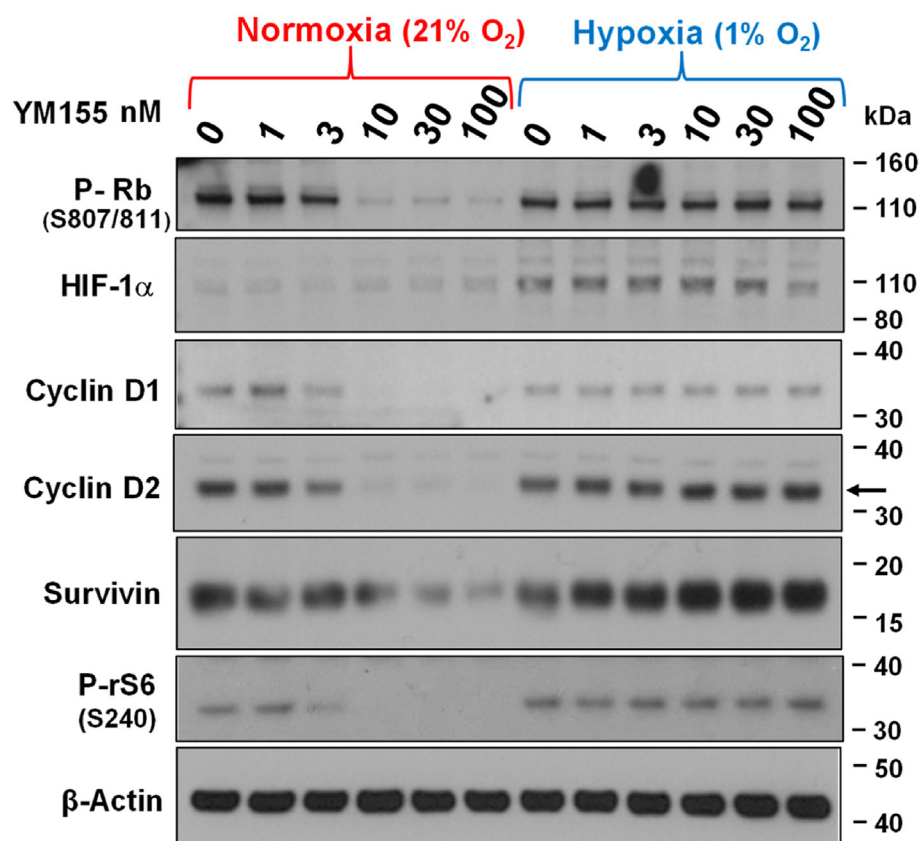
Fig. 2. Effect of hypoxia on the ability of YM155 control cell cycle regulators in PC-3 cells. PC-3 cells were allowed to attach to 6-well dishes for 24 h under normal atmospheric oxygen (21% O_2), the cells were pre-incubated for 24 h in 1% or 21% O_2 before treatment with various doses of YM155 or vehicle for 8 h continuously under the same conditions. Expression of P–Rb (S807/811), Cyclin D1, Cyclin D2, Survivin, HIF-1α, and β-Actin were determined by Western blot analysis, as described in Materials and Methods. The data shown are representative of three independent experiments.

melanoma (Lewis et al., 2009), and Her2-negative metastatic breast cancer (Clemens et al., 2015), where it was shown to be generally well tolerated but have modest anti-tumor activity when administered alone (Giaccone et al., 2009; Lewis et al., 2009) or in combination with docetaxel, paclitaxel, carboplatin, and rituximab (Tolcher et al., 2011; Clemens et al., 2015; Papadopoulos et al., 2016; Kelly et al., 2013). Since then, multiple *in vivo* studies have focused on exploiting other drug combinations or drug delivery strategies to improve the effectiveness of YM155 in various preclinical models (Baspinar et al., 2019; Gholizadeh et al., 2018; Dai et al., 2018; Woo et al., 2017; Radic-Sarikas et al., 2017). To date, no study has explored the role of the tumor microenvironment or tumor hypoxia on the anti-cancer activity of YM155. Our report here represents the first study to assess the role of hypoxia on the anti-cancer activity of YM155. Our data support that hypoxia may play a prominent role in the limited clinical responsiveness of tumors to YM155, and provide novel insight that may enable improved clinical strategies for the therapeutic use of YM155 and structurally related analogs.

2. Materials and Methods

2.1. Materials

Sources were: YM155, BEZ-235 (Selleck Chemicals); rabbit anti-Survivin IgG (#AF886) (R&D Systems); rabbit anti-P-Rb (S807/811, #9308), mouse anti-Cyclin D1 (#2926), rabbit anti-Mcl-1(#5453), rabbit anti-P-p70S6K1 (T389, #9205), rabbit anti-Raptor (#4978, #4972) rabbit anti-P-Raptor (S792, #2083), rabbit anit-HIF-1α (#3716), rabbit anti-HIF-2α (#7096), rabbit anti-VHL (#2738), rabbit anti-P-AMPKα (T172, #2535), rabbit anti-Cyclin D1 (sc-753), rabbit anti-Cyclin D2 (sc-593), mouse anti-P-rS6 (S240, sc-293143), mouse anti-rS6 (sc-74459), mouse anti-GAPDH (sc-51907), mouse anti-AMPK-α1 (39881) (Santa Cruz Biotechnologies, Inc.); mouse anti-β-actin (#A-5441), dimethyoxalylglycine (400091), deferoxamine mesylate (D9533) (Sigma-Aldrich,

Inc.); DMEM/F12 (Media Tech); characterized fetal bovine serum (FBS) (HyClone); Roscovitine (LC labs).

2.2. Cell culture

The human PC-3, DU145, LNCaP, CWR22Rv1, and 786-O cell lines were obtained from American Type Culture Collection (ATCC), RCC4 cells were obtained from Sigma-Aldrich, and C4-2 cells were from Leland Chung's lab. PC-3, DU-145, LNCaP, C4-2, and RCC4 cells were maintained in DMEM/Ham's F-12 medium (1:1, v/v) with 5% FBS. The LNCaP cells were maintained in plates coated with poly-D-lysine as before (Shankar et al., 2016). All cell lines were maintained in 5% CO_2 at 37 °C.

2.3. Cell growth/Viability assay

Cells were plated overnight in 12 well dishes at a density of 10,000 cells/1 mL/well in a Forma Scientific cell culture incubator (37° C, 5% CO_2, 21% O_2). Those dishes were maintained in that incubator or placed in a C21 BioSpherix hypoxia chamber (37° C, 5% CO_2, 0.5–2.5% O_2) within that incubator and then either immediately or 24 h later treated with YM155 (0.1–1000 nM). Following three days of drug treatment, cells were stained with crystal violet, as previously described (Song et al., 2013). The data were plotted and evaluated for statistical significance and the half-maximal inhibitory concentrations (IC_{50}) of YM155 were calculated using GraphPad Prism Software. Each point on the graph represents the average of triplicate determinations ± one standard error from the mean (S.E.). P-values were calculated by Student's t-test (two-tailed).

2.4. Western blotting

Cells (10^5 cells/ml DMEM/F12 + 5% FBS) were plated in 6-well dishes (2 ml/well), allowed overnight to adhere to plastic, and then
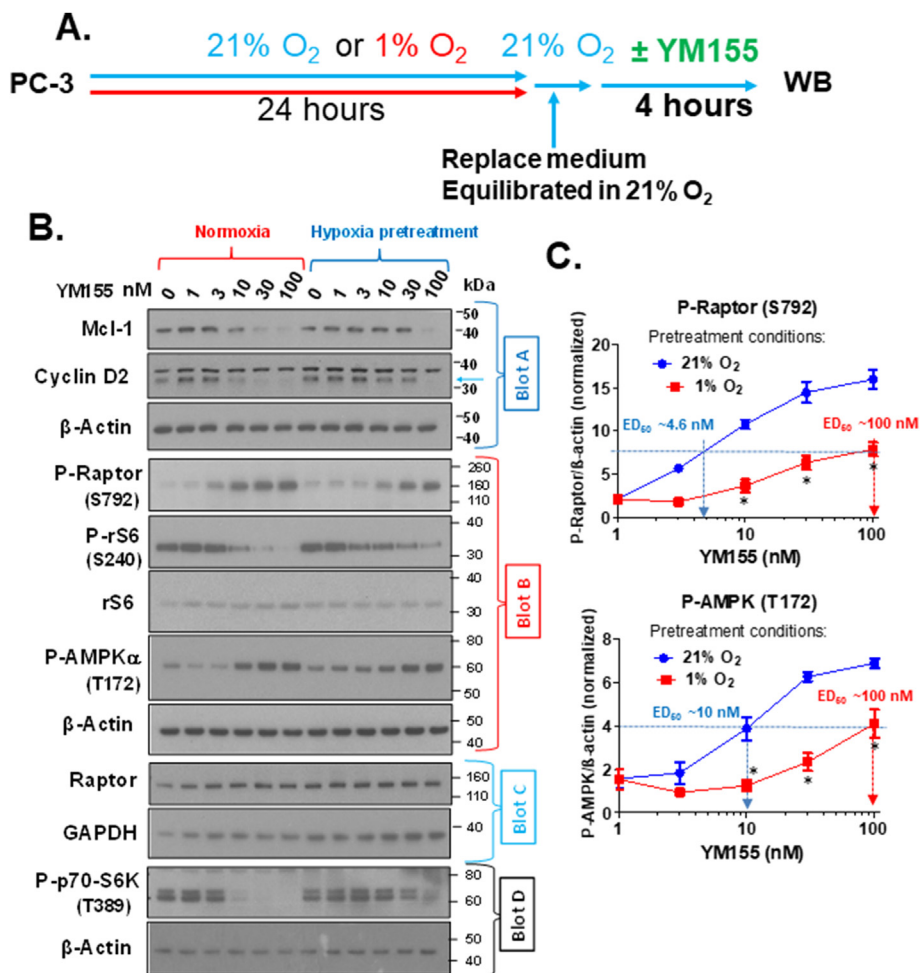
Fig. 3. Pre-treatment with hypoxia alone suppresses early signaling responses in PC-3 elicited by YM155 in 21% O_2. PC-3 cells were allowed to attach to 6-well dishes for 24 h under normal atmospheric oxygen (21% O_2), the cells were pre-incubated for 24 h in 1% or 21% O_2 before treatment with various doses of YM155 or vehicle for 4 h in 21% O_2 (A). Expression of Mcl-1, Cyclin D2, P-Raptor (S792), Raptor, P-rS6 (S240), rS6, P-AMPKα (T172) Survivin, P-p70S6K (T389), and β-Actin were determined by Western blot analysis (B), as described in Materials and Methods. C) The ED_{50} of YM155 on the phosphorylation of Raptor and AMPK in cells pre-treated for 24 h with 21% O_2 versus 1% O_2 was quantified by Image J. The data shown are representative of two independently conducted experiments. The graphs in C were generated by normalization to β-actin values after the background phosphorylation induced by hypoxia was subtracted for the comparative analysis of ED_{50}s of YM155. Each data point represents the average of 5 replicates (5 composite scans from 3 different blots representing biological replicates) ± SE. Statistical significance (p-values) was determined by Student's t-test (two-tailed). *$p < 0.05$.

treated as indicated. Following treatment, wells were washed twice with 2 ml of PBS, lysed with 120 ul of RIPA buffer containing protease inhibitor cocktail (Song et al., 2013), and clarified lysates were processed for Western blot analysis, as detailed before (Song et al., 2013). Protein expression was determined by Western analysis using 4–12% Bis-Tris NuPAGE[TM] gels, SDS-MES or SDS-MOPS running buffer (200 V, 4° C), 0.45 μm nitrocellulose membranes, NuPAGE[TM] Transfer Buffer, Novex Sharp Pre-stained Protein Standards and chemiluminescent autoradiography on film (Fuji Medical 100 NIF). To ensure equal protein loading, protein concentrations of samples were determined by a BCA protein assay (96-well format), using an 8-point BSA standard curve run in duplicate and a Tecan plate reader. Unknown samples were the average of triplicate determinations. Equal loading and transfer were confirmed by staining membranes with Ponceau S. The NIH Image J software was used to quantify signals generated from Western Blots. Such quantification was done using the average of five film exposures within the linear densitometric range (from at least 3 blots, each representing a different experiment or biological replicate). Densitometric values were normalized to that of β-Actin controls.

2.5. Lentiviral-mediated silencing of HIF-1α and -2α

HIFs were silenced with pLKO.1 lentiviral shRNA constructs (HIF-1α: TRCN0000003808, TRCN0000003809, TRCN0000003810; HIF2α: TRCN0000003803, TRCN0000003807, TRCN0000003804) obtained from Sigma, Inc. To produce viral supernatants, we transfected subconfluent monolayers of HEK293T cells with pLKO.1 sh-RNA, pMD2.G, and pCMV-dR8.74 (Shankar et al., 2016). Viral supernatants were collected

between 24 and 72 h after transfection. PC-3 and 786-O cells were transduced overnight with viral supernatant (MOI = 0.5) in the presence of 8 μg/ml polybrene for 24 h, and 24 h after replacing with fresh growth medium, cells were selected by treatment with 1.5 μg/ml puromycin for four days or until 100% death of the non-transduced cells.

3. Results

3.1. Cytotoxicity of YM155 on prostate cancer cells is suppressed by hypoxia

Recent findings support that the tumor microenvironment plays a vital role in responses to cancer therapy and drug resistance (Jing et al., 2019). A critical component of the tumor microenvironment is hypoxia. Here we tested the effect of hypoxia on the biological activity of YM155 in prostate cancer cell lines. We first compared the cytostatic/cytotoxic activity of YM155 on the PC-3 prostate cancer cell line under atmospheric oxygen (21% O_2) versus hypoxic (1% O_2) conditions (Fig. 1a). For this experiment, untreated cells in all groups were allowed 24 h to adhere to plastic in the same incubator at 21% O_2 and then treated with various doses of YM155. We returned one set of plates to the same 37°C incubator set at 21% O_2 + 5% CO_2, and another set of duplicate-treated plates to a hypoxic chamber within that incubator set at 1% O_2 + 5% CO_2. After 72 h, cell growth was assessed by a crystal violet staining growth assay. Under these conditions, although hypoxia slightly suppressed the overall growth of vehicle control-treated cells, it significantly increased the half-maximal inhibitory concentration (IC_{50}) of YM155 from 1.7 nM to about 12 nM, representing a ~7-fold increase (Fig. 1a).
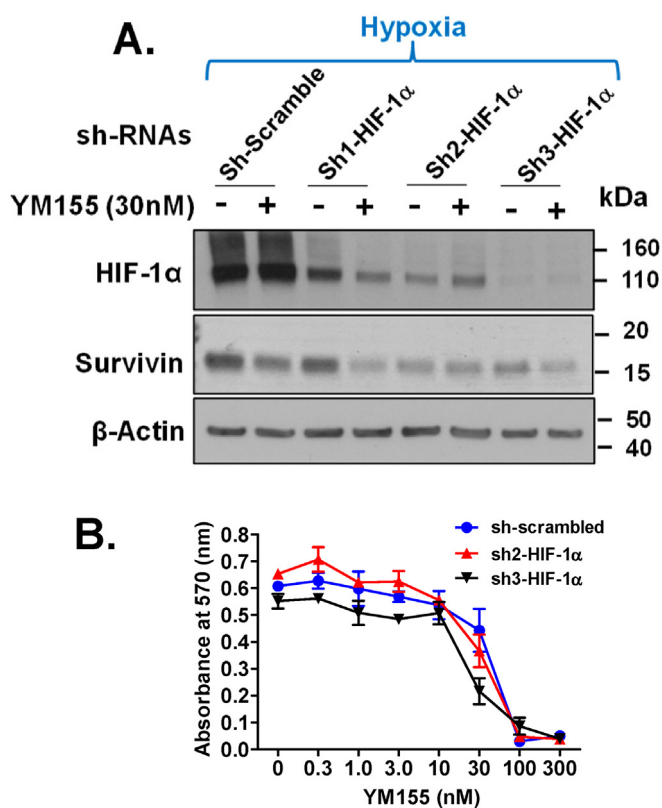
Fig. 4. Impact of HIF-1α on the ability of hypoxia to YM155 to control growth regulators and suppress the growth of PC-3 cells. PC-3 cells stably silenced for the expression of HIF-1α by lentiviral mediated transduction of HIF-1α shRNAs or scrambled control shRNA were allowed to attach overnight to 6-well **(A)** and 12-well **(B)** dishes in 21% O$_2$. Cells were then pre-incubated for 24 h with 1% or 21% O$_2$ before treatment with various doses of YM155 or vehicle for 4 h (A) or 72 h **(B)** with 1% or 21% O$_2$. The dependence of HIF-1α on the impact of hypoxia on YM155 responses was assessed by Western blot analysis **(A)** and crystal violet growth assay **(B)**. Data points in panel B represent the average of biological triplicates ± SE.

The above data opened the possibility that a hypoxia-inducible response was involved in shifting the dose-response curve of YM155 to the right. We tested this by setting up another growth assay identically as above except PC-3 cells were cultured with 1% O$_2$ versus 21% O$_2$ for 24 h before treatment with YM155. Such pre-treatment further increased the IC$_{50}$ of YM155 on PC-3 cells from 1.8 nM to 26.8 nM, representing a ~15-fold increase in IC$_{50}$ (Fig. 1b). Of note, the shape and slope of the dose-response curves generated at 21% O$_2$ were comparable to that generated at 1% O$_2$. These results suggest that hypoxia preconditions PC-3 cells to repress the cytotoxic activity of YM155 by increasing its IC$_{50}$ without altering the magnitude of its suppression. We also similarly determined alterations in the IC$_{50}$ of YM155 on the growth of PC-3 cells incubated in 2.5% O$_2$ (Figs. 1c), 5% O$_2$, and 0.5% O$_2$ (Fig. 1d, Table 1). Culturing PC-3 cells with 2.5% O$_2$ and 0.5% O$_2$ increased the IC$_{50}$ of YM155 by 10-fold and 62.5-fold, respectively, whereas culturing cells with 5% O$_2$ did not alter this drug's IC$_{50}$ (Table 1). In contrast to YM155, hypoxia (1% O$_2$) did not alter the IC$_{50}$ of the cyclin-dependent kinase inhibitor Roscovitine on growth arrest of PC-3 cells under identical conditions (Supplementary Fig. S1). Taken together, these results support that a physiologically hypoxic response, as exemplified by the induction of HIF-1α and HIF-2α protein levels, selectively increases the IC$_{50}$ of YM155 on PC-3 cells.

We next tested whether hypoxia (1% O$_2$, 24-h pre-incubation) similarly increases the IC$_{50}$ of YM155 on the cytotoxicity of four other prostate cancer cell lines (Table 2). We found that hypoxia increases the IC$_{50}$ of YM155, ranging from >6.8-fold to 25-fold, on growth suppression/cell death of LNCaP, DU145, C4-2, and CWR22RV1 (22RV1) cells, suggesting that hypoxia universally increases the IC$_{50}$ of YM155 necessary to suppress prostate cancer cell growth.

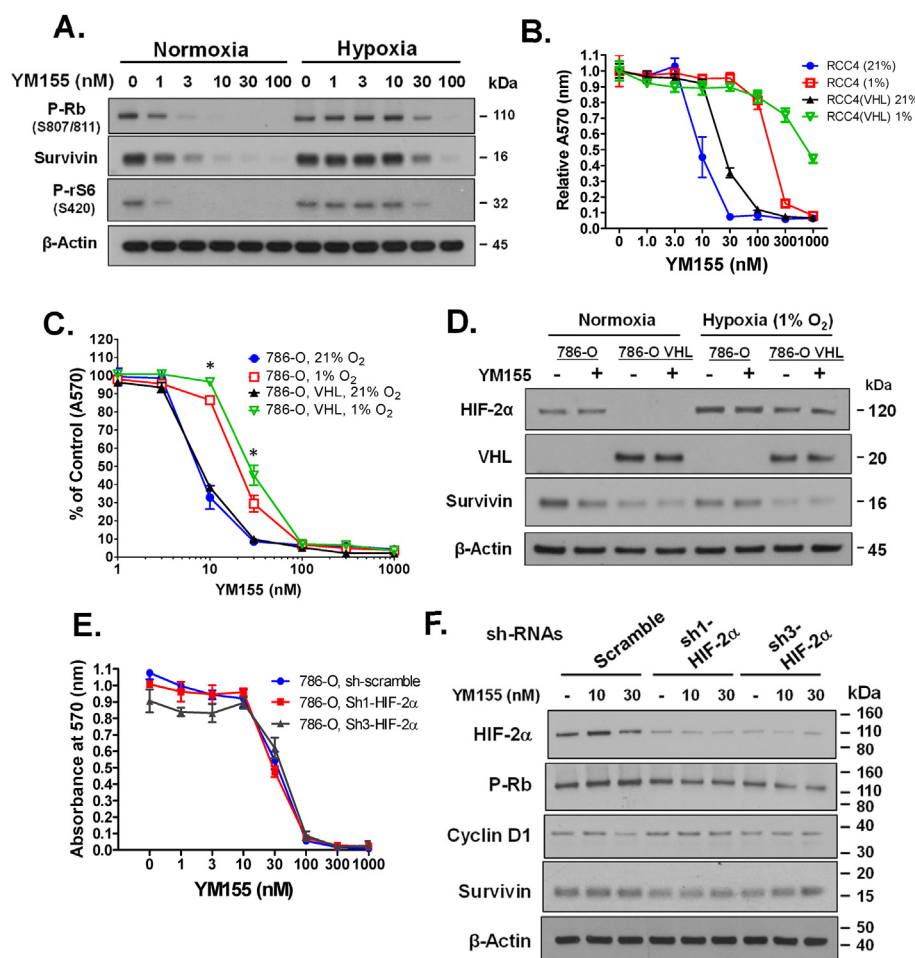### 3.2. Effect of hypoxia on early responses of prostate cancer cells to YM155

We recently reported that suppression of the mammalian target of rapamycin complex 1 (mTORC1) is an early response to YM155, leading to translational suppression of numerous proteins, including Survivin and Cyclin Ds, the latter responses of which promotes Rb activation (Danielpour et al., 2019). We next sought to determine whether hypoxia also represses those early responses to YM155. To test this, we incubated PC-3 cells in 1% O$_2$ versus 21% O$_2$ for 24 h before 8 h treatment with various doses of YM155. Western blot analysis of cells revealed that hypoxia robustly blocked the ability of YM155 to suppress the phosphorylation of ribosomal protein S6 (rS6) at S240 (a phosphorylation site exclusively targeted by the mTORC1 activated kinase S6K1 (Danielpour et al., 2019)), the levels of Cyclin D1, Cyclin D2, and Survivin, and the phosphorylation of Rb at S807/811 (Fig. 2). Under these conditions, hypoxia shifted the ED$_{50}$ of those changes from ~3 nM to >100 nM, representing >30-fold increased ED$_{50}$ of YM155. These results suggest that hypoxia represses early signaling responses of cells to YM155.

We previously entertained the possibility that YM155's ability to activate AMPK and hence suppress mTORC1 may be the consequence of oxidative stress (Danielpour et al., 2019), based on a hypothesis that YM155 promotes oxidative DNA damage (Wani et al., 2018), and that activation of AMPK was the readout of this response (Eliopoulos et al., 2016). This possibility would suggest that the early responses to YM155, such as activation of AMPK, suppression of mTORC1, and suppression of protein synthesis, are dependent on the level of cellular oxygen during YM155 treatment. To test this possibility, we pre-conditioned PC-3 cells with 1% or 21% O$_2$ for 24 h and then placed both cultures in the same incubator containing 21% O$_2$, where we then treated them with various doses of YM155 or vehicle for 4 h. We ensured there was no lag in the time of oxygenation of cells by replacing the medium of all cultures with fresh medium equilibrated in 21% O$_2$ before adding YM155. After 4 h of YM155 treatment, cells were processed for Western blot analysis of early signaling responses to YM155 (Fig. 3A). Our results demonstrated that cells pre-incubated under hypoxia were significantly less responsive to YM155 (Fig. 3B) with a 10- to 20-fold increase in ED$_{50}$ (Fig. 3C) as assessed by densitometric scanning using the NIH Image J software. Based on this, we hypothesized that the suppressive effect of hypoxia on YM155 responses was due to a hypoxia-inducible factor (HIF), belonging to the family of transcription factors that mediate cellular responses to hypoxia (Hajizadeh et al., 2019). The reduced impact of hypoxia on YM155 responses in Fig. 3 compared to Fig. 2 is consistent with the very rapid degradation of HIF-αs at 21% O$_2$ (Batie et al., 2019).

3.3. Effect of HIFs in cellular responses to YM155

We employed two strategies to test the role of HIFs in mediating the hypoxia-driven reduction in sensitivity to YM155. The first strategy involved silencing the expression of HIF-1α and HIF-2α with shRNAs, and the second strategy involved using syngeneic cells proficient in or lacking pVHL, the E3 ubiquitin ligase essential for proteasome-mediated degradation of HIFs under normoxia (Qian et al., 2018). We used three unique shRNAs for silencing the expression of HIF-1α in PC-3 cells. All three shRNAs effectively silenced HIF-1α induced by hypoxia (Fig. 4). Loss of HIF-1α by each of these shRNAs was also accompanied by decreased expression of Survivin. The two constructs that most strongly silenced HIF-1α did not significantly enhance the effectiveness of YM155 to suppress the expression of Survivin (Fig. 4A) or growth (Fig. 4B) of PC-3 cells, suggesting that HIF-1α alone does not play a significant role in driving suppression of YM155 activity by hypoxia.

The RCC4 renal cell carcinoma cell line is null for the tumor suppressor gene pVHL, promoting the constitutive expression of HIFs under

Fig. 5. Impact of hypoxia on YM155 responses in renal carcinoma cells deficient or proficient in pVHL. A) VHL-null RCC4 cells were first allowed to attach to 6-well dishes for 24 h under normal atmospheric oxygen (21% O_2), they were then pre-incubated for 24 h in 1% or 21% O_2 and thereafter treated with various doses of YM155 or vehicle for 24 h in 1% or 21% O_2. B) VHL null RCC4 cells and VHL expressing RCC4 cells were first allowed to attach to 12-well dishes for 24 h under normal atmospheric oxygen (21% O_2), they were then pre-incubated for 24 h in 1% or 21% O_2 and subsequently treated with YM155 or vehicle for 72 h with their respective levels of O_2. C, D) VLH proficient and null 786-O cells were first allowed to attach to 12-well (C) or 6-well (D) dishes for 24 h under normal atmospheric oxygen (21% O_2), then pre-incubated for 24 h in 1% or 21% O_2 and subsequently treated with YM155 or vehicle for 72 h (C) or 24 h (D) in their respective levels of O_2. E, F) VHL-null 786-O cells stably silenced for HIF-2α by lentiviral-mediated transduction of HIF-2α shRNAs versus scramble control shRNA were first allowed to attach to 12-well (E) or 6-well (F) dishes for 24 h under normal atmospheric oxygen (21% O_2), they were then pre-incubated for 24 h in 1% or 21% O_2 and subsequently treated with YM155 or vehicle for 72 h (E) or 24 h (F) with their respective levels of O_2. Cells were analyzed for cell growth by crystal violet growth assay (B, C, E) or alteration of signaling responses by Western blot (A, D, F). Data points in panels B, D, and E represent the average of triplicate biological determinations ± SE. Statistical significance (p-values) was determined by Student's t-test. *p < 0.01 comparisons are for differences between 1% versus 21% O_2 for both VHL proficient and deficient cells.

normoxia. Nevertheless, in RCC4 cells hypoxia robustly (~30-fold increase in IC_{50}) suppresses the ability of YM155 to activate Rb, suppress the expression of Survivin, and suppress the phosphorylation of rS6 at S240 (Fig. 5A). Hypoxia similarly increased the IC_{50} of YM155 on growth suppression of RCC4 cells (Fig. 5B). Interestingly, enforced over-expression of pVHL slightly increased rather than decreased the IC_{50} of YM155 on suppressing the growth of RCC4 cells independent of the status of hypoxia (Fig. 5B), consistent with the possibility that the suppressive effect of hypoxia on the activity of YM155 is independent of HIFs. Hypoxia also increased the IC_{50} of YM155 for growth suppression of the VLH-null 786-O renal cell carcinoma cell line, although the fold suppression was not as robust as that of RCC4 cells (Fig. 5C). Overexpression of pVHL did not noticeably alter the IC_{50} of YM155 on growth suppression of 786-O cells under normoxia. However, under hypoxia pVHL overexpression seemed to modestly increase the IC_{50} of YM155 on growth suppression of 786-O cells (Fig. 5C).

Unlike RCC4 cells that express HIF-1α and HIF-2α, 786-O cells express HIF-2α but not HIF-1α (Hu et al., 2003). Western blot analysis demonstrated that hypoxia induces the expression of HIF-2α by ~2-fold in pVHL-null 786-O cells, allowing the possibility that this induction of HIF-2α may account for the impact of hypoxia on the responsiveness of 786-O cells to YM155. We, therefore, assessed the effect of HIF-2α on YM155 responses by silencing HIF-2α expression in 786-O cells. Two different shRNAs that effectively silenced HIF-2α expression did not enhance the sensitivity of 786-O cells (cultured under hypoxia) to YM155, as assessed by growth suppression (Fig. 5D) or early gene responses (Fig. 5E). Together, these results support that HIF-1α and HIF-2α do not play a significant role in the repressive effect of hypoxia on cellular responses to YM155.

To further characterize how hypoxia may induce resistance to YM155, we treated PC-3 cells for 3 h with two highly cell-permeable hypoxic mimetics, deferoxamine mesylate (DFX) (0.2 mM) (Woo et al., 2006) and dimethyloxalylglycine (DMOG) (1 mM) (Hagg and Wennstrom, 2005) versus vehicle control, before a 2 h co-treatment with YM155 (100 nM) of vehicle (see Fig. 6a for experimental design). Cells were then subjected to Western blot analysis for various proteins including HIF-1α, VEGFR2, P-Raptor (S792), P-rS6 (S240), P-AMPKα (T172), total AMPKα1, and Cyclin D1 (Fig. 6). Although this brief treatment with those mimetics helped PC-3 cells to achieve a hypoxic response as evidenced by a robust induction of HIF-1α, they did not depress the effectiveness of YM155 to alter early signaling responses. Of note, YM155 suppressed the expression of AMPKα1, which is consistent with our previous study (Danielpour et al., 2019). These results are in contrast to the robust loss in YM155 (100 nM)-induced early responses that occurred in PC-3 cells following 24 h of hypoxia-pretreatment (Fig. 2). Based on the mechanism of action of those inhibitors (Woo et al., 2006; Hagg and Wennstrom, 2005; Recalcati et al., 2015; Paul et al., 2017), the results of Fig. 6 suggest that these early signaling responses by YM155 are independent of monooxygenases, dioxygenases, and other proteins with iron-containing co-factors.

4. Discussion

Our study here represents the first report that hypoxia robustly diminishes the cytotoxic/cytostatic action of YM155 on cancer cells, and that hypoxia represses cellular responses to YM155 including all the early ones we have studied to date. Our data, showing that pre-conditioning cells to hypoxia decreases their responsiveness to YM155 even when
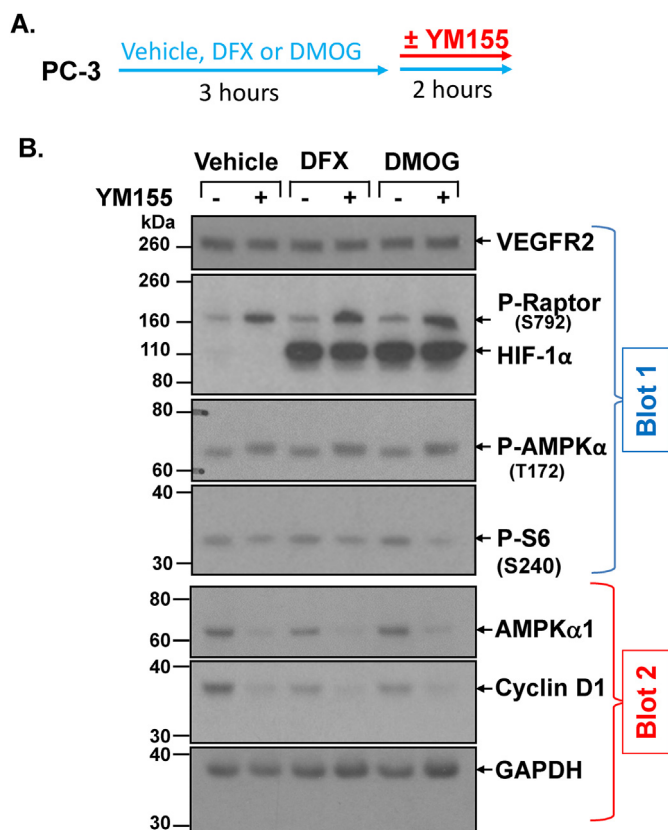
Fig. 6. YM155 alters early cellular responses independent of cellular delivery of oxygen. PC-3 cells were allowed to attach to 6-well dishes for 24 h under normal culture conditions, the cells were then treated with 0.2 mM deferoxamine mesylate (DFX), 1 mM dimethyloxalylglycine (DMOG), or water (vehicle). Following 180 min treatment cells received 100 nM YM155 or vehicle, and after an additional 120 min, cells were harvested for Western blot analysis (A). Expression of P-Raptor (S792), HIF-1α, VEGFR2, P-rS6 (S240), P-AMPKα (T172), AMPKα1, Cyclin D1, and GAPDH was determined by Western blot analysis. The data shown are representative of two independent experiments.

cells are returned to atmospheric oxygen levels during the YM155 treatment period (Fig. 3), suggest that hypoxia causes a fundamental alteration in cells that reduces their responsiveness to YM155. Moreover, short treatment with the hypoxia mimetics DFX and DMOG, the former of which chelates iron and interferes with the utilization of oxygen by proteins with iron-containing cofactors in mitochondria, such as mono-oxygenases and dioxygenases (Woo et al., 2006; Hagg and Wennstrom, 2005; Recalcati et al., 2015; Paul et al., 2017), did not repress early cell signaling responses to YM155 (Fig. 6). Taken together, these results support that the ability of hypoxia to suppress cellular responsiveness to YM155 is dependent on some type of hypoxia-inducible mechanism rather than a direct lack of the availability of oxygen as a substrate.

Normal eukaryotic cells are equipped with various mechanisms to protect them from necrotic cell death caused by severe hypoxia or anoxia (Majmundar et al., 2010). In the best-understood mechanism, hypoxia stabilizes HIF-1α, which then dimerizes with HIF-1β to form a transcriptional complex that binds to the hypoxia response element (HRE) of the VEGF promoter, thereby transcriptionally inducing the expression of VEGF (Tirpe et al., 2019). VEGF then binds to VEGF receptors on endothelial cells, thus promoting the growth of new blood vessels that supply hypoxic tissues with oxygen and nutrients. Hypoxia similarly stabilizes HIF-2α and HIF-3α, each of which dimerizes with HIF-1β to interact with HREs of numerous other genes. While HIF-1α is expressed in nearly all tissues, HIF-2α and particularly HIF-3α are more limited in their tissue expression patterns. Under normoxia, HIF-αs get hydroxylated on
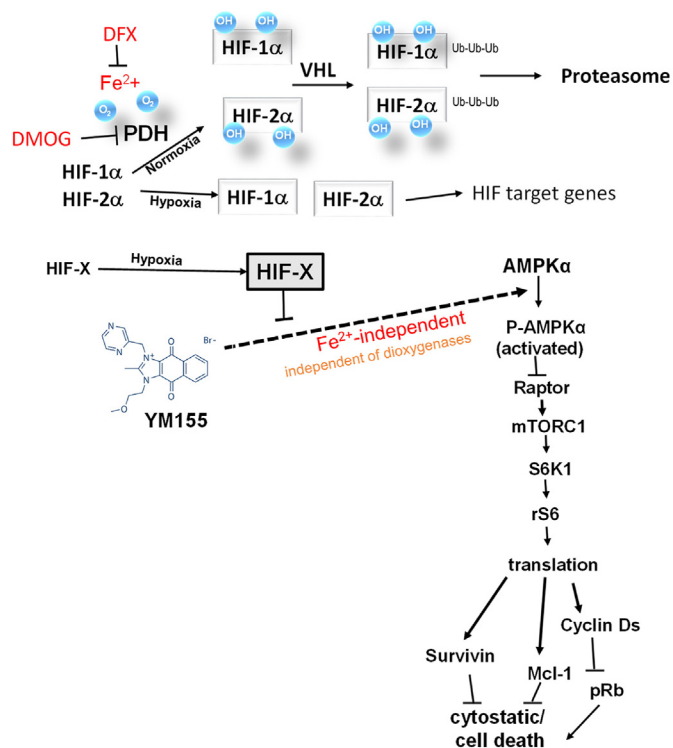

Fig. 7. Summary of a model describing the potential mechanism by which hypoxia suppresses cellular responses to YM155. Our study support that hypoxia, through a HIF-1α and HIF-2α-independent mechanism, inhibits the cytostatic/cytotoxic responses to YM155 in part by inhibiting the activation of AMPK and subsequently reversing YM155's suppression of a previously reported downstream signaling cascade, including the activity of mTORC1, S6K1, and rS6 and translation of Survivin, Mcl-1, and Cyclin Ds (Danielpour et al., 2019). The ability of hypoxia to repress YM155-mediated loss of phosphorylated pRB can be explained by changes in Cyclin Ds that partner with cyclin-dependent kinases to inactivate pRB through the phosphorylation of pRB at S807/811 (Danielpour et al., 2019). The iron chelator DFX, which induces the expression of HIF-1α by repressing proline hydroxylation of HIF-1α, does not antagonize early responses to YM155, suggesting that YM155 activates AMPK through an iron-independent mechanism. We hypothesize that an unknown hypoxia-inducible factor (designated HIF-X) suppresses cellular response to YM155.

conserved proline residues by proline hydroxylases (PHDs), members of the dioxygenase family of oxidizing enzymes (Minervini et al., 2015). Hydroxylated HIF-αs are then targeted for proteasomal degradation following their polyubiquitination by the von Hippel-Lindau (pVHL) E3 ubiquitin ligase complex (Qian et al., 2018), an important tumor suppressor whose loss of function is associated with the appearance of tumors arising in multiple organs (Mikhail and Singh, 2020). Our data in the current study support that HIFs do not play a role in the mechanism by which hypoxia suppresses cellular responsiveness to YM155 (Figs, 4, 5, 7).

Currently, we do not know the alteration in cellular behavior that hypoxia triggers to render cells less responsive to YM155. Although HIFs represent the best-studied mechanism by which hypoxia impacts cellular responses through gene regulation, many reports confirm the critical roles of HIF-independent cellular responses to hypoxia (Vozdek et al., 2018; Fortenbery et al., 2018; Ahmed et al., 2018; Park et al., 2016). Importantly, a recent study provided strong evidence that hypoxia re-programs global changes in gene expression by rapidly modifying chromatin methylation through a HIF-independent mechanism (Batie et al., 2019). This study disclosed that histone demethylases characterized by a JmjC domain (i.e., KDM5A-D) could function as O₂ sensors, wherein O₂ inhibits their activity. As such, low O₂ de-represses those demethylases, particularly KDM5A, leading to enhanced trimethylation

of histone H3 at various residues.

Hypoxia is well known to activate nitroreductases through a HIF-independent mechanism (Brown and Wilson, 2004). Such nitroreductase activity has been widely used to visualize tumor hypoxia through reduction of the fluorochrome pimonidazole (Aguilera and Brekken, 2014) and to selectively activate cancer prodrugs (Brown and Wilson, 2004). Nitroreductases may potentially inactivate YM155 or the direct target of YM155. However, nitroreductases are instantly inactivated under normoxia and thus cannot explain our results in Fig. 3 in which the entire duration of cell treatment with YM155 occurred in 21% O_2.

Whether hypoxia squelches the responsiveness of cancer cells to YM155 through any of the above HIF-independent mechanisms remains to be examined. Our data, demonstrating that hypoxia inhibits the onset of the earliest reported cellular responses to YM155 (i.e., activation of AMPK), support the possibility that a cellular alteration imposed by hypoxia may interfere with the initiation of cellular response to YM155 (see Fig. 7 for our overall model). In our model, we hypothesize that an unknown hypoxia-inducible factor, designated as HIF-X, is responsible for the suppression of cellular response to YM155. We previously showed that YM155 activates AMPK by promoting the phosphorylation of AMPKα at T172, and that activation of AMPK by YM155 inactivates Raptor through phosphorylating Raptor at S792 (Danielpour et al., 2019), which is a phosphorylation site exclusively targeted by AMPK. Inactivation of Raptor, which is an obligate subunit of the mTORC1 complex (mTORC1), inactivates mTORC1. Inactivated mTORC1 promotes the inactivation of S6K1 (seen by loss of phosphorylation of S6K1 at T389), and thereby decreases phosphorylation of S6K1's target, rS6 at S240. Through this and other mechanisms, suppression of mTORC1 promotes inhibition of the translation of various proteins required for cell growth and survival, such as Survivin, Mcl-1, and Cyclin Ds. As expected, hypoxia suppressed the activation of AMPK by YM155, and thus all responses downstream of AMPK (Figs. 2, 3 and 7). Given that cellular uptake of YM155 requires a cationic transporter, the cellular response to hypoxia may involve an alteration in the expression or activity of that transporter. Alternatively, hypoxia may alter the immediate intracellular target of YM155 or disrupt its interaction with YM155. Further work in understanding the molecular mechanism by which hypoxia decreases the responsiveness of cancer cells to YM155 may disclose new opportunities to improve the effectiveness of this drug or its derivatives in targeting cancer.

Irrespective of the mechanism by which hypoxia represses the responsiveness of tumor cells to YM155, strategies that promote the selective delivery of oxygen to tumors are likely to significantly enhance the anti-cancer therapeutic efficacy of YM155. Recent efforts hold much promise for efficiently delivering oxygen to tumors to counteract the tumor-promoting and drug-resistance effects of hypoxia. A recent study reported effective tumor delivery of oxygen and enhanced therapeutic action of cabazitaxel via an artificial oxygen carrier that employed liposomes loaded with hemoglobin and cabazitaxel (Jiang et al., 2019). In the latest study, Zhang et al. (2019) developed a new nano-carrier, named FeSiAuO, capable of delivering both drug and oxygen to the tumor microenvironment under visible light radiation. The latter represents a new and innovative version of photodynamic therapy that targets tumors through two independent hits: improved drug delivery/action and suppressing tumor progression through targeted down-regulation of HIF. These and other artificial oxygen delivery systems hold promising strategies to enhance the therapeutic efficacy of YM155 on solid tumors.

CRediT authorship contribution statement

David Danielpour: Supervision, Conceptualization, Formal analysis, Funding acquisition, Resources, Data curation, Writing – original draft, Writing – review & editing. **Sarah Corum:** Conceptualization, Data curation, Writing – review & editing. **Scott M. Welford:** Conceptualization, Writing – review & editing. **Eswar Shankar:** Conceptualization, Data curation, Formal analysis, Writing – review & editing.

Declaration of competing interest

The authors declare the following financial interests/personal relationships which may be considered as potential competing interests:

David Danielpour reports was provided by Case Western Reserve University. David Danielpour reports a relationship with Case Western Reserve University that includes:. David Danielpour has patent pending to none. none.

Appendix A. Supplementary data

Supplementary data to this article can be found online at https://doi.org/10.1016/j.crphar.2021.100076.

References

Aguilera, K.Y., Brekken, R.A., 2014. Hypoxia studies with pimonidazole in vivo. Bio. Protoc. 4.

Ahmed, E.M., Bandopadhyay, G., Coyle, B., Grabowska, A., 2018. A HIF-independent, CD133-mediated mechanism of cisplatin resistance in glioblastoma cells. Cell. Oncol. 41, 319–328.

Aoyama, Y., Kaibara, A., Takada, A., Nishimura, T., Katashima, M., Sawamoto, T., 2013. Population pharmacokinetic modeling of sepantronium bromide (YM155), a small molecule survivin suppressant, in patients with non-small cell lung cancer, hormone refractory prostate cancer, or unresectable stage III or IV melanoma. Invest. N. Drugs 31, 443–451.

Baek, J.H., Jang, J.E., Kang, C.M., Chung, H.Y., Kim, N.D., Kim, K.W., 2000. Hypoxia-induced VEGF enhances tumor survivability via suppression of serum deprivation-induced apoptosis. Oncogene 19, 4621–4631.

Baspinar, Y., Erel-Akbaba, G., Kotmakci, M., Akbaba, H., 2019. Development and characterization of nanobubbles containing paclitaxel and survivin inhibitor YM155 against lung cancer. Int. J. Pharm. 566, 149–156.

Batie, M., Frost, J., Frost, M., Wilson, J.W., Schofield, P., Rocha, S., 2019. Hypoxia induces rapid changes to histone methylation and reprograms chromatin. Science 363, 1222–1226.

Brown, J.M., 1990. Tumor hypoxia, drug resistance, and metastases. J. Natl. Cancer Inst. 82, 338–339.

Brown, J.M., Wilson, W.R., 2004. Exploiting tumour hypoxia in cancer treatment. Nat. Rev. Cancer 4, 437–447.

Chang, B.H., Johnson, K., LaTocha, D., Rowley, J.S., Bryant, J., Burke, R., Smith, R.L., Loriaux, M., Muschen, M., Mullighan, C., Druker, B.J., Tyner, J.W., 2015. YM155 potently kills acute lymphoblastic leukemia cells through activation of the DNA damage pathway. J. Hematol. Oncol. 8, 39.

Clemens, M.R., Gladkov, O.A., Gartner, E., Vladimirov, V., Crown, J., Steinberg, J., Jie, F., Keating, A., 2015. Phase II, multicenter, open-label, randomized study of YM155 plus docetaxel as first-line treatment in patients with HER2-negative metastatic breast cancer. Breast Cancer Res. Treat. 149, 171–179.

Dai, C.H., Shu, Y., Chen, P., Wu, J.N., Zhu, L.H., Yuan, R.X., Long, W.G., Zhu, Y.M., Li, J., 2018. YM155 sensitizes non-small cell lung cancer cells to EGFR-tyrosine kinase inhibitors through the mechanism of autophagy induction. Biochim. Biophys. Acta (BBA) - Mol. Basis Dis. 1864, 3786–3798.

Danielpour, D., Gao, Z., Zmina, P.M., Shankar, E., Shultes, B.C., Jobava, R., Welford, S.M., Hatzoglou, M., 2019. Early cellular responses of prostate carcinoma cells to sepantronium bromide (YM155) involve suppression of mTORC1 by AMPK. Sci. Rep. 9, 11541.

Das, V., Bruzzese, F., Konecny, P., Iannelli, F., Budillon, A., Hajduch, M., 2015. Pathophysiologically relevant in vitro tumor models for drug screening. Drug Discov. Today 20, 848–855.

Detmar, M., Brown, L.F., Berse, B., Jackman, R.W., Elicker, B.M., Dvorak, H.F., Claffey, K.P., 1997. Hypoxia regulates the expression of vascular permeability factor/vascular endothelial growth factor (VPF/VEGF) and its receptors in human skin. J. Invest. Dermatol. 108, 263–268.

Eliopoulos, A.G., Havaki, S., Gorgoulis, V.G., 2016. DNA damage response and autophagy: a meaningful partnership. Front. Genet. 7, 204.

Feng, W.Y.A., Ueda, T., 2013. YM155 induces caspase-8 dependent apoptosis through downregulation of survivin and Mcl-1 in human leukemia cells. Biochem. Biophys. Res. Commun. 435 (1), 52–57.

Feng, W., Yoshida, A., Ueda, T., 2013. YM155 induces caspase-8 dependent apoptosis through downregulation of survivin and Mcl-1 in human leukemia cells. Biochem. Biophys. Res. Commun. 435, 52–57.

Fortenbery, G.W., Sarathy, B., Carraway, K.R., Mansfield, K.D., 2018. Hypoxic stabilization of mRNA is HIF-independent but requires mtROS. Cell. Mol. Biol. Lett. 23, 48.

Gholizadeh, S., Dolman, E.M., Wieriks, R., Sparidans, R.W., Hennink, W.E., Kok, R.J., 2018. Anti-GD2 immunoliposomes for targeted delivery of the survivin inhibitor sepantronium bromide (YM155) to neuroblastoma tumor cells. Pharm. Res. (N. Y.) 35, 85.

Giaccone, G., Zatloukal, P., Roubec, J., Floor, K., Musil, J., Kuta, M., van Klaveren, R.J., Chaudhary, S., Gunther, A., Shamsili, S., 2009. Multicenter phase II trial of YM155, a small-molecule suppressor of survivin, in patients with advanced, refractory, non-small-cell lung cancer. J. Clin. Oncol. 27, 4481–4486.

Glaros Tg, S.L., Mullendore, M.E., Smith, B., Morrison, B.L., Newton, D.L., 2012. The "survivin suppressants" NSC 80467 and YM155 induce a DNA damage response. Cancer Chemother. Pharmacol. 70 (1), 207–212.

Griner, L.M., Gampa, K., Do, T., Nguyen, H., Farley, D., Hogan, C.J., Auld, D.S., Silver, S.J., 2018. Generation of high-throughput three-dimensional tumor spheroids for drug screening. JoVE.

Hagg, M., Wennstrom, S., 2005. Activation of hypoxia-induced transcription in normoxia. Exp. Cell Res. 306, 180–191.

Hajizadeh, F., Okoye, I., Esmaily, M., Ghasemi Chaleshtari, M., Masjedi, A., Azizi, G., Irandoust, M., Ghalamfarsa, G., Jadidi-Niaragh, F., 2019. Hypoxia inducible factors in the tumor microenvironment as therapeutic targets of cancer stem cells. Life Sci. 237, 116952.

Hu, C.J., Wang, L.Y., Chodosh, L.A., Keith, B., Simon, M.C., 2003. Differential roles of hypoxia-inducible factor 1alpha (HIF-1alpha) and HIF-2alpha in hypoxic gene regulation. Mol. Cell Biol. 23, 9361–9374.

Iwasa, T., Okamoto, I., Takezawa, K., Yamanaka, K., Nakahara, T., Kita, A., Koutoku, H., Sasamata, M., Hatashita, E., Yamada, Y., Kuwata, K., Fukuoka, M., Nakagawa, K., 2010. Marked anti-tumour activity of the combination of YM155, a novel survivin suppressant, and platinum-based drugs. Br. J. Cancer 103, 36–42.

Iwasa T, O.I., Suzuki, M., Nakahara, T., Yamanaka, K., Hatashita, E., Yamada, Y., Fukuoka, M., Ono, K., Nakagawa, K., 2008. Radiosensitizing effect of YM155, a novel small-molecule survivin suppressant, in non-small cell lung cancer cell lines. Clin. Cancer Res. 14 (20), 6496–6504.

Jiang, J., Tang, Y.L., Liang, X.H., 2011. EMT: a new vision of hypoxia promoting cancer progression. Cancer Biol. Ther. 11, 714–723.

Jiang, M.S., Yin, X.Y., Qin, B., Xuan, S.Y., Yuan, X.L., Yin, H., Zhu, C., Li, X., Yang, J., Du, Y.Z., Luo, L.H., You, J., 2019. Inhibiting hypoxia and chemotherapy-induced cancer cell metastasis under a valid therapeutic effect by an assistance of biomimetic oxygen delivery. Mol. Pharm. 16, 4530–4541.

Jing, X., Yang, F., Shao, C., Wei, K., Xie, M., Shen, H., Shu, Y., 2019. Role of hypoxia in cancer therapy by regulating the tumor microenvironment. Mol. Cancer 18, 157.

Kelly, R.J., Thomas, A., Rajan, A., Chun, G., Lopez-Chavez, A., Szabo, E., Spencer, S., Carter, C.A., Guha, U., Khozin, S., Poondru, S., Van Sant, C., Keating, A., Steinberg, S.M., Figg, W., Giaccone, G., 2013. A phase I/II study of sepantronium bromide (YM155, survivin suppressor) with paclitaxel and carboplatin in patients with advanced non-small-cell lung cancer. Ann. Oncol. 24, 2601–2606.

Lewis, K.D., Samlowski, W., Ward, J., Catlett, J., Cranmer, L., Kirkwood, J., Lawson, D., Whitman, E., Gonzalez, R., 2009. A multi-center phase II evaluation of the small molecule survivin suppressor YM155 in patients with unresectable stage III or IV melanoma. Invest. N. Drugs 29, 161–166.

Majmundar, A.J., Wong, W.J., Simon, M.C., 2010. Hypoxia-inducible factors and the response to hypoxic stress. Mol. Cell. 40, 294–309.

Mikhail, M.I., Singh, A.K., 2020. Von Hippel Lindau Syndrome.

Minematsu, T., Iwai, M., Sugimoto, K., Shirai, N., Nakahara, T., Usui, T., Kamimura, H., 2009. Carrier-mediated uptake of 1-(2-methoxyethyl)-2-methyl-4,9-dioxo-3-(pyrazin-2-ylmethyl)-4,9-dihydro-1H-napht ho[2,3-d]imidazolium bromide (YM155 monobromide), a novel small-molecule survivin suppressant, into human solid tumor and lymphoma cells. Drug Metab. Dispos. 37, 619–628.

Minervini, G., Quaglia, F., Tosatto, S.C., 2015. Insights into the proline hydroxylase (PHD) family, molecular evolution and its impact on human health. Biochimie 116, 114–124.

Na, Y.S., Yang, S.J., Kim, S.M., Jung, K.A., Moon, J.H., Shin, J.S., Yoon, D.H., Hong, Y.S., Ryu, M.H., Lee, J.L., Lee, J.S., Kim, T.W., 2012. YM155 induces EGFR suppression in pancreatic cancer cells. PLoS One 7, e38625.

Nakahara, T., Kita, A., Yamanaka, K., Mori, M., Amino, N., Takeuchi, M., Tominaga, F., Hatakeyama, S., Kinoyama, I., Matsuhisa, A., Kudoh, M., Sasamata, M., 2007. YM155, a novel small-molecule survivin suppressant, induces regression of established human hormone-refractory prostate tumor xenografts. Cancer Res. 67, 8014–8021.

Nakahara, T., Kita, A., Yamanaka, K., Mori, M., Amino, N., Takeuchi, M., Tominaga, F., Kinoyama, I., Matsuhisa, A., Kudoh, M., Sasamata, M., 2011. Broad spectrum and potent antitumor activities of YM155, a novel small-molecule survivin suppressant, in a wide variety of human cancer cell lines and xenograft models. Cancer Sci. 102, 614–621.

Osinsky, S., Zavelevich, M., Vaupel, P., 2009. Tumor hypoxia and malignant progression. Exp. Oncol. 31, 80–86.

Papadopoulos, K.P., Lopez-Jimenez, J., Smith, S.E., Steinberg, J., Keating, A., Sasse, C., Jie, F., Thyss, A., 2016. A multicenter phase II study of sepantronium bromide (YM155) plus rituximab in patients with relapsed aggressive B-cell Non-Hodgkin lymphoma. Leuk. Lymphoma 57, 1848–1855.

Park, J.Y., Jung, J.Y., Kim, H.J., Bae, I.H., Kim, D.Y., Lee, T.R., Shin, D.W., 2016. Hypoxia leads to abnormal epidermal differentiation via HIF-independent pathways. Biochem. Biophys. Res. Commun. 469, 251–256.

Paul, B.T., Manz, D.H., Torti, F.M., Torti, S.V., 2017. Mitochondria and Iron: current questions. Expet Rev. Hematol. 10, 65–79.

Qian, H., Zou, Y., Tang, Y., Gong, Y., Qian, Z., Wei, G., Zhang, Q., 2018. Proline hydroxylation at different sites in hypoxia-inducible factor 1alpha modulates its interactions with the von Hippel-Lindau tumor suppressor protein. Phys. Chem. Chem. Phys. 20, 18756–18765.

Radic-Sarikas, B., Halasz, M., Huber, K.V.M., Winter, G.E., Tsafou, K.P., Papamarkou, T., Brunak, S., Kolch, W., Superti-Furga, G., 2017. Lapatinib potentiates cytotoxicity of YM155 in neuroblastoma via inhibition of the ABCB1 efflux transporter. Sci. Rep. 7, 3091.

Recalcati, S., Gammella, E., Cairo, G., 2015. New perspectives on the molecular basis of the interaction between oxygen homeostasis and iron metabolism. Hypoxia 3, 93–103.

Shankar, E., Song, K., Corum, S.L., Bane, K.L., Wang, H., Kao, H.Y., Danielpour, D., 2016. A signaling network controlling androgenic repression of c-Fos protein in prostate adenocarcinoma cells. J. Biol. Chem. 291, 5512–5526.

Shukla, S.K., Mulder, S.E., Singh, P.K., 2018. Hypoxia-mediated in vivo tumor glucose uptake measurement and analysis. Methods Mol. Biol. 1742, 107–113.

Song, K., Shankar, E., Yang, J., Bane, K.L., Wahdan-Alaswad, R., Danielpour, D., 2013. Critical role of a survivin/TGF-beta/mTORC1 axis in IGF-I-mediated growth of prostate epithelial cells. PLoS One 8, e61896.

Sorensen, B.S., Horsman, M.R., 2020. Tumor hypoxia: impact on radiation therapy and molecular pathways. Front. Oncol. 10, 562.

Tang, H., Shao, H., Yu, C., Hou, J., 2011. Mcl-1 downregulation by YM155 contributes to its synergistic anti-tumor activities with ABT-263. Biochem. Pharmacol. 82, 1066–1072.

Tao, Y.F., Lu, J., Du, X.J., Sun, L.C., Zhao, X., Peng, L., Cao, L., Xiao, P.F., Pang, L., Wu, D., Wang, N., Feng, X., Li, Y.H., Ni, J., Wang, J., Pan, J., 2012. Survivin selective inhibitor YM155 induce apoptosis in SK-NEP-1 Wilms tumor cells. BMC Cancer 12, 619.

Tirpe, A.A., Gulei, D., Ciortea, S.M., Crivii, C., Berindan-Neagoe, I., 2019. Hypoxia: overview on hypoxia-mediated mechanisms with a focus on the role of HIF genes. Int. J. Mol. Sci. 20.

Tolcher, A.W., Quinn, D.I., Ferrari, A., Ahmann, F., Giaccone, G., Drake, T., Keating, A., de Bono, J.S., 2011. A phase II study of YM155, a novel small-molecule suppressor of survivin, in castration-resistant taxane-pretreated prostate cancer. Ann. Oncol. 23, 968–973.

Vozdek, R., Long, Y., Ma, D.K., 2018. The receptor tyrosine kinase HIR-1 coordinates HIF-independent responses to hypoxia and extracellular matrix injury. Sci. Signal. 11.

Wagner, V., Hose, D., Seckinger, A., Weiz, L., Meissner, T., Reme, T., Breitkreutz, I., Podar, K., Ho, A.D., Goldschmidt, H., Kramer, A., Klein, B., Raab, M.S., 2014. Preclinical efficacy of sepantronium bromide (YM155) in multiple myeloma is conferred by down regulation of Mcl-1. Oncotarget 5, 10237–10250.

Wang, Q., Chen, Z., Diao, X., Huang, S., 2011. Induction of autophagy-dependent apoptosis by the survivin suppressant YM155 in prostate cancer cells. Cancer Lett. 302, 29–36.

Wang, Y.F., Zhang, W., He, K.F., Liu, B., Zhang, L., Zhang, W.F., Kulkarni, A.B., Zhao, Y.F., Sun, Z.J., 2014. Induction of autophagy-dependent cell death by the survivin suppressant YM155 in salivary adenoid cystic carcinoma. Apoptosis 19, 748–758.

Wani, T.H., Surendran, S., Jana, A., Chakrabarty, A., Chowdhury, G., 2018. Quinone-based antitumor agent sepantronium bromide (YM155) causes oxygen-independent redox-activated oxidative DNA damage. Chem. Res. Toxicol. 31, 612–618.

Wani, T.H., Chowdhury, G., Chakrabarty, A., 2021. Generation of reactive oxygen species is the primary mode of action and cause of survivin suppression by sepantronium bromide (YM155). RSC Med. Chem. 12, 566–578.

Woo, K.J., Lee, T.J., Park, J.W., Kwon, T.K., 2006. Desferrioxamine, an iron chelator, enhances HIF-1alpha accumulation via cyclooxygenase-2 signaling pathway. Biochem. Biophys. Res. Commun. 343, 8–14.

Woo, S.M., Min, K.J., Seo, B.R., Seo, Y.H., Jeong, Y.J., Kwon, T.K., 2017. YM155 enhances ABT-737-mediated apoptosis through Mcl-1 downregulation in Mcl-1-overexpressed cancer cells. Mol. Cell. Biochem. 429, 91–102.

Xu, Q., Mackay, R.P., Xiao, A.Y., Copland, J.A., Weinberger, P.M., 2021. Ym155 induces oxidative stress-mediated DNA damage and cell cycle arrest, and causes programmed cell death in anaplastic thyroid cancer cells. Int. J. Mol. Sci. 22.

Zhang, X., Wang, X., Xu, R., Ji, J., Xu, Y., Han, M., Wei, Y., Huang, B., Chen, A., Zhang, Q., Li, W., Wang, J., Li, X., Qiu, C., 2018. YM155 decreases radiation-induced invasion and reverses epithelial-mesenchymal transition by targeting STAT3 in glioblastoma. J. Transl. Med. 16, 79.

Zhang, Z., Niu, N., Gao, X., Han, F., Chen, Z., Li, S., Li, J., 2019. A new drug carrier with oxygen generation function for modulating tumor hypoxia microenvironment in cancer chemotherapy. Colloids Surf. B Biointerfaces 173, 335–345.